Heliyon 11 (2025) e42098

Contents lists available at ScienceDirect

Heliyon

journal homepage: www.cell.com/heliyon

Research article

Identification of signaling networks associated with lactate modulation of macrophages and dendritic cells

Rapeepat Sangsuwan [a,b], Bhasirie Thuamsang [a], Noah Pacifici [a], Phum Tachachartvanich [c], Devan Murphy [d], Abhineet Ram [d], John Albeck [d], Jamal S. Lewis [a,e,*]

[a] Department of Biomedical Engineering, University of California, Davis, CA, 95616, USA
[b] Laboratory of Natural Products, Chulabhorn Research Institute, Bangkok, 10210, Thailand
[c] Laboratory of Environmental Toxicology, Chulabhorn Research Institute, Bangkok, 10210, Thailand
[d] Department of Molecular and Cell Biology, University of California, Davis, CA, 95616, USA
[e] J. Crayton Pruitt Family Department of Biomedical Engineering, University of Florida, FL, 32611, USA

ARTICLE INFO

Keywords:
Lactate
Immunomodulatory
Dendritic cells
Macrophages
Tumor microenvironment

ABSTRACT

The advancement in the understanding of cancer immune evasion has manifested the development of cancer immunotherapeutic approaches such as checkpoint inhibitors and interleukin agonists. Although cancer immunotherapy breakthroughs have demonstrated improved potency for cancer treatment, only a fraction of patients effectively respond to these treatments. Moreover, there is compelling evidence indicating that cancer cells develop a unique microenvironment through adaptive metabolic reprogramming, which aberrantly modulates host immunity to evade immunosurveillance. As part of the tumor cell adaptive metabolic switch, lactate is produced and released into the tumor environment. Recent studies have shown that lactate significantly modulates immune functions, especially in innate immune cells. Dendritic cells (DCs) and macrophages (MΦs) are specialized antigen-presenting cells serving as key players in innate immunity and anticancer-associated immune responses. Although most studies have shown that lactate affects immune phenotypes (e.g., surface protein expression and cytokine production), the cell signaling network mediated by lactate is not fully understood. In the present study, we identified the key signaling pathways in bone marrow-derived DCs and MΦs that were changed by cancer-relevant concentrations of lactate. First, transcriptome analysis was used to guide notable signaling pathways mediated by lactate. Subsequently, biomolecular techniques, including immunoblotting, flow cytometry, and immunofluorescence imaging were performed to corroborate the changes in these key signaling pathways at the protein level. The results indicated that lactate differentially impacted the biochemical networks of DCs and MΦs. While lactate mainly altered STAT3, ERK, and p38 MAPK signaling cascades in DCs, the STAT1 and GSK-3β signaling in MΦs were the major pathways significantly impacted by lactate. This study identifies key biochemical pathways in innate immune cells that are impacted by lactate, which advances our understanding of the interplay between the tumor microenvironment and innate immunity.

* Corresponding author. J. Crayton Pruitt Family Department of Biomedical Engineering, University of Florida, FL, 32611, USA.
E-mail addresses: jamlewis@ucdavis.edu, JLewis@bme.ufl.edu (J.S. Lewis).

https://doi.org/10.1016/j.heliyon.2025.e42098
Received 8 July 2024; Received in revised form 16 January 2025; Accepted 17 January 2025
Available online 28 January 2025

1. Introduction

Dendritic cells (DCs) and macrophages (MΦs) are two key players in anticancer-associated immune responses. The immunological functions of DCs and MΦs in the tumor microenvironment (TME) profoundly govern the ability of the host immune system to eradicate cancer cells [1–4]. The detection of tumor-associated antigens by these two immune surveilling cells—DCs and MΦs—is the first key event in anticancer immunity [1–3]. Upon antigen recognition, DCs and MΦs orchestrate the adaptive immune responses by providing T-cell-receptor specific ligands and costimulatory molecules for the activation and expansion of anti-tumor T cells [1–4]. These actions collectively lead to a complete eradication of tumor-initiating cells by effector T cells at the tumor site [1–3]. However, it has been shown that metabolic reprogramming by cancer cells markedly generates a unique TME, which modulates host immunity to 'down arms', assumes more immunosuppressive states, and abdicates their roles in immune surveillance [5].

Metabolic reprogramming has been considered a key characteristic of cancer, required for tumor transformation and progression [6–9], enabling cancers to adapt to stimuli from TME through plasticity in nutrient acquisition and utilization [6–9]. Cancer cells can undergo metabolic reprogramming, reverting to a mode where their metabolic activities mainly rely on glycolysis instead of oxidative phosphorylation [10]. As part of this adaptive metabolic switch, a glucose molecule is converted to two molecules of pyruvate, which is subsequently reduced to lactate by a lactate dehydrogenase (LDH) enzyme [5]. Further, lactate is subsequently exported and/or secreted through a monocarboxylate transporter [5]. With the high extent of glycolytic flux in cancer metabolic reprogramming, lactate is extensively produced and secreted into the TME at relatively high concentrations ranging from 4 to 50 mM, whereas the normal physiological level of lactate is approximately 1.5–3 mM [9,11–17]. Over the last decade, several lines of evidence have indicated that lactate is not just a product of glycolysis but rather plays a critical role in immunomodulation, particularly in surveilling cells including DCs and MΦs. For example, our previous in vitro study [18] as well as other findings done in breast cancer tissues or multicellular tumor spheroids [19–22] have shown that high lactate levels subverted DCs to a more tolerogenic phenotype as evidenced by reduced inflammatory cytokine production and impaired ability for antigen presentation. It has been shown in animal studies that the suppression of major histocompatibility complex (MHC) antigen presentation caused by elevated levels of lactate dampened the priming of T cells by tolerogenic DCs, which in turn, mitigated the initiation of anti-tumor responses in lung tumor tissues [23]. The immunomodulatory effect of lactate is also coherently observed in MΦs. Likewise, cancer cell-derived lactate promoted an immunosuppressive phenotype in MΦs, inducing M2 polarization. The levels of colony-stimulating factor 1 receptor (CSF1R), CD163, *Vegf* and Arg*1*, as well as other immunosuppressive markers in MΦs were increased in response to higher concentrations of lactic acid derived from various kinds of cancers including skin, colon, breast, head, neck, cervical, and pancreatic cancers [24–31]. Moreover, a plethora of studies have now reported on lactate as an immunosuppressive agent for various immune cells [20–22,24–27,29,32–35]. For instance, lactate inhibits the cytotoxic immune response of NK cells and promotes cancer progression and metastasis [32]. Brand et al. revealed that lactic acid produced by LDHA in glycolysis produced acidification, impaired cytokine production such as IFN-γ and reduced activity of tumor-infiltrating T cells and NK cells, therefore promoting the tumor growth in melanoma patients [32]. Yet, there is conflicting evidence which indicates that lactate either acts as an immune stimulator or has no effect on immune cells. Factors attributable to this discrepancy include different experimental designs, cell types, and confounding factors, such as acidity. Indeed, acidity itself was found to improve antigen presentation of DCs as exposure of hydrochloric acid to DCs enhanced endocytosis and increased the expression of MHC-II, CD11c, and costimulatory molecules CD80 and CD86, as well as improved MHC class I-restricted antigen presentation by DCs [36]. Conversely, the acidity of TME was reported to induce G protein-coupled receptor (GPCR) expression and promote M2 polarization [37]. Moreover, our group previously uncovered the role of lactate in preventing TAK-1 phosphorylation in the canonical NF-κB pathway in DCs challenged with LPS after lactate treatment [18]. Together with our following study, DC and MΦ modulation after lactate treatment even without LPS challenge indicated that other networks were involved in the immunomodulation effect of lactate. Altogether, it is imperative to unveil the full effect of lactate, and its biomolecular network in innate immune cells, particularly DCs and MΦs. Our understanding of the immunophenotypes associated with the tumor microenvironment and their molecular underpinnings would profit the fight against cancer tremendously.

While the use of human immune cells is often constrained due to availability, complexity and invasiveness, mice serve as a valuable alternative in biomedical studies, allowing for translational research relevant to humans. Murine bone marrow (BM)-derived cells are particularly robust for studying immune functions, largely due to their accessibility and ability to be freshly isolated [38]. Recently, we investigated the immunomodulatory effect of lactate on murine BMDCs and BMMΦs under buffered conditions [39]. It is important to note that the concentration of lactate used in the current study mirrors levels observed in cancer [9,11–17]. This is significant, as it enables the findings from murine cells to be extrapolated to the tumor microenvironment in human cancers. Interestingly, lactate significantly dampened the lipopolysaccharide (LPS)-induced DC maturation and reduced IL-12 production [39]. In addition, lactate also consistently promoted immunosuppressive phenotypes in MΦs towards M2 polarization by upregulating the expression of several M2 markers [39]. Although most studies on the immunomodulatory effects of lactate have focused on phenotype characterization including protein surface markers and cytokine productions, molecular signaling changes relating to anticancer-associated immune responses due to elevated lactate in these two key innate immune cells have not been fully unveiled. To address this knowledge gap, we performed transcriptome analysis followed by several molecular biological assays including immunoblotting, flow cytometry, and immunofluorescence staining. Collectively, this study provides insights into the molecular mechanisms of lactate immune modulation and the ability of this special molecule to retrain critical signaling pathways in innate immune cells. The implications are quite significant as we seek to uncover more efficacious therapies to counteract cancer.

2. Materials and methods

2.1. Animal protocol

C57BL/6J mice, 6–12 weeks old, were obtained from Jackson Laboratory (Bar Harbor, ME). All animals were maintained in a specific pathogen-free environment in the University of California, Davis facilities and handled in accordance with the experimental protocol (#21139) approved by the University of California Institutional Animal Care and Use Committee (IACUC). This work was performed during the 2020–2022 period under the aforementioned approved IACUC protocol.

2.2. Generation of BM-derived dendritic cells and macrophages

Dendritic cells and MΦs were isolated from male and female C57BL/6J mice in accordance with the University of California, Davis IACUC-approved guidelines, following a previously published protocol [39]. Briefly, mice were euthanized using CO_2 followed by cervical dislocation. Bone marrow cells were harvested by extracting the tibias and femurs, then using a 25-gauge needle to flush the interior of the long bones with RPMI medium supplemented with 10% (v/v) fetal bovine serum (FBS, Corning), 100 U/mL penicillin/streptomycin (Hyclone), 1 mM sodium pyruvate (Lonza), 1% (v/v) nonessential amino acids (100X, Lonza). The resulting cell suspension was passed through a 70 μm strainer (Becton Dickinson) and centrifuged at 300 r.c.f. for 5 min. The filtered cells were treated with ACK lysis buffer (Lonza) for 5 min at room temperature to lyse red blood cells, followed by centrifugation at 300 r.c.f. for 5 min to isolate leukocytes. The leukocytes were then resuspended in DMEM/F-12 (1:1) medium with 10% (v/v) FBS (Corning), 100 U/mL penicillin/streptomycin (Hyclone), 1 mM sodium pyruvate (Lonza), 1% (v/v) nonessential amino acids (100X, Lonza), and a differentiation-specific factor: either 10 ng/mL GM-CSF (R&D Systems) for DC media or 10% (v/v) L-929 supplement for MΦ media, as previously described [39]. The cells were seeded into tissue culture flasks and incubated for 48 h to enable attachment of differentiated cells. On day 2, only nonadherent cells were collected, moved to low-attachment plates, and cultured in fresh DC or MΦ media for precursor cell expansion. On day 6, adhesion and proliferation of the cells were facilitated by transferring them to tissue culture plates. Following differentiation, the cells were exposed to either 50 mM sLA or control media for 48 h at 37 °C, following previously established protocols [39]. They were then processed for RNA extraction, Western blot analysis, and immunofluorescence staining.

2.3. RNA isolation procedures and sequencing

RNA was harvested from DCs and MΦs (1 million cells/well) exposed to either control media or 50 mM sLA, using the same protocol mentioned in 2.2. TRIzol reagent (1 mL/well, Thermo Fisher Scientific) was added to the cells, followed by chloroform addition to facilitate phase separation. RNA was precipitated from the aqueous phase using a 1:1 ratio of ethanol. The isolated nucleic acid material was purified, DNAse-treated, and concentrated using an RNA Clean & Concentrator kit (Zymo Research). The samples were subjected to quality assessment using LabChip GX nucleic acid analyzer at the UC Davis DNA core. The top-scoring technical replicates were selected and sent to the DNA Core via 3′-Tag-Seq (QuantSeq) Library Preparation and Illumina HiSeq 4000. Gene expression levels between the sLA-treated and control groups were analyzed in R using the limma-voom pipeline, and adjusted p-values were calculated using the Benjamini-Hochberg procedure. For each comparison, the log fold change (Log2FC) and adjusted p-value levels for each comparison were used for further analysis.

2.4. Downstream analysis of differentially expressed genes

The genes for each comparison group were threshold-filtered by an adjusted p-value less than or equal to 0.05 and a magnitude of Log2FC greater than 0.5. The significant genes of sLA vs. control comparisons in DCs and MΦs were compared using an online bioinformatics tool (https://bioinformatics.psb.ugent.be/webtools/Venn/) to yield a condensed list of 63 differentially expressed genes. Enrichment analysis of this gene set was performed using an online Enrichr tool (https://maayanlab.cloud/Enrichr/). This analysis was used to check for significant terms within Wikipathways and Gene Ontology Biological Processes enrichment lists for potential key pathway candidates. For graphical representation of gene expression via volcano plots and heatmaps, R packages EnhancedVolcano and pheatmap were used, respectively. Visualization of pathway expression change was performed via Omicsoft bioinformatics software.

2.5. Western blot analysis

Cells were exposed to either control media or 50 mM sLA, using the same protocol mentioned in 2.2. Following the treatment, cells were lysed and protein lysate samples were collected and quantified based on previously published protocol [40]. Sodium dodecyl sulfate-polyacrylamide gel electrophoresis (SDS-PAGE) was conducted on a mini gel apparatus, using 7.5% or 4–20% precast polyacrylamide gels, Mini-PROTEAN® TGX™ (Bio-rad #4561023, #4561094). The sample and electrode buffers were prepared according to the Laemmli procedure. Protein electrophoresis samples were heated at 95 °C for 10 min with 2-mercaptoethanol to reduce disulfide bonds. The membranes were subsequently blocked overnight at 4 °C in 10 mL of tris-buffered saline with 0.1% (v/v) Tween-20 (TBST), supplemented with 5% (w/v) bovine serum albumin (Roche). The membrane was incubated with each primary antibody targeting phosphorylated STAT1 (p-STAT1, Tyr701, D4A7, Cell signaling technology (CST) #7649), p-STAT2 (Tyr690, CST #4441), p-STAT3 (Ser727, CST #9134), p-SAPK/JNK (Thr183/Tyr185, 81E11, CST #4668), p-SAPK/JNK (Thr183/Tyr185, 98F2, CST #4671), p-NF-κB

p65 (Ser536, 93H1, CST #3033), β-Catenin (Ser45, D2U8Y, CST #19807), p-Akt (Ser473, CST #9271), p-Akt (Thr308, D25E6, CST #13038), p-Akt (Ser473, D9E, CST #4060), Akt (pan) (C67E7, CST #4691), p-PTEN (Ser380, CST #9551), p-GSK-3β (Ser9, D85E12, CST #5558), p-c-Raf (Ser259, CST #9421), p-PDK1 (Ser241, C49H2, CST #3438), p-p44/42 MAPK (Erk1/2, Thr202/Tyr204, D13.14.4E, CST #4370), p-p38 MAPK (Thr180/Tyr182, D3F9, CST #4511), and β-actin (CST #4967). The membrane was then washed with TBST, and a secondary antibody was incubated for 1 h. The membrane was then washed with TBST followed by chemiluminescence detection using HRP substrate (SuperSignal West Pico/Femto Chemiluminescent 98 Substrate (Pierce)). Membrane imaging was performed on a Gel Doc System (Bio-Rad). The levels of protein expression normalized to the actin were determined using ImageJ.

2.6. Flow cytometry

Cells were exposed to either control media or 50 mM sLA, using the same protocol mentioned in 2.2. After sLA exposure for 48 h, Fcγ receptors on DCs and MΦs were blocked by incubating the cells with antibodies against CD16/CD32 (Fcγ III/II Receptor) (clone 2.4G2, IgG2b, k); (BD Pharmingen #553142) in 5% FBS (v/v) for 20 min at 4 °C. This was followed by a 25-min staining with cell-specific markers: anti-CD11c (N418) (Thermo Fisher Scientific #63-0114-82) for DCs; anti-F4/80(BM8.1) (CST #88154) for MΦ). The cells were washed twice and subsequently stained with UV Zombie dye (BioLegend #423107) to identify viable cells. For intracellular staining, cells were fixed and permeabilized using an intracellular fixation and permeabilization buffer set (Thermo Fisher Scientific). They were then stained with antibodies targeting phosphorylated proteins: p-STAT1 (Tyr701, 58D6, CST #8009), p-STAT3 (Tyr705, Thermo Fisher Scientific #12-9033-42), p-GSK-3β (Ser9, D85E12, CST #5558), p-p44/42 MAPK (Erk1/2, Thr202/Tyr204, 197G2, CST #13148), p-p38 MAPK alpha (Thr180, Tyr182, Thermo Fisher Scientific #MA5-36913). The stained cells were analyzed using an Attune NxT Flow Cytometer (Thermo Fisher Scientific), collecting at least 10,000 events per sample. Data were processed using Attune software (Thermo Fisher Scientific). Singlets of live cell populations were gated based on UV Zombie dye staining (Fig. S1). Cells were further identified using specific markers—CD11c for DCs and F4/80 for MΦs—and their respective protein expressions were analyzed. Positive staining gates were established using fluorescence-minus-one (FMO) controls.

2.7. Immunofluorescence staining

Cells were seeded at a density of 7500 cells/well in 96-well plates. After 24 h, cells were treated with 50 mM sLA or media with no sLA for 48 h (At least 10 wells per treatment condition). At 48 h post-sLA treatment, cells were fixed with 2% (v/v) paraformaldehyde final concentration in phosphate-buffered saline (PBS) for 15 min. Cells were then permeabilized with 100% methanol for 10 min, washed with PBS, and blocked with blocking buffer (1% (w/v) BSA in PBS with 0.1% (v/v) Tween [PBST]). for 1 h at room

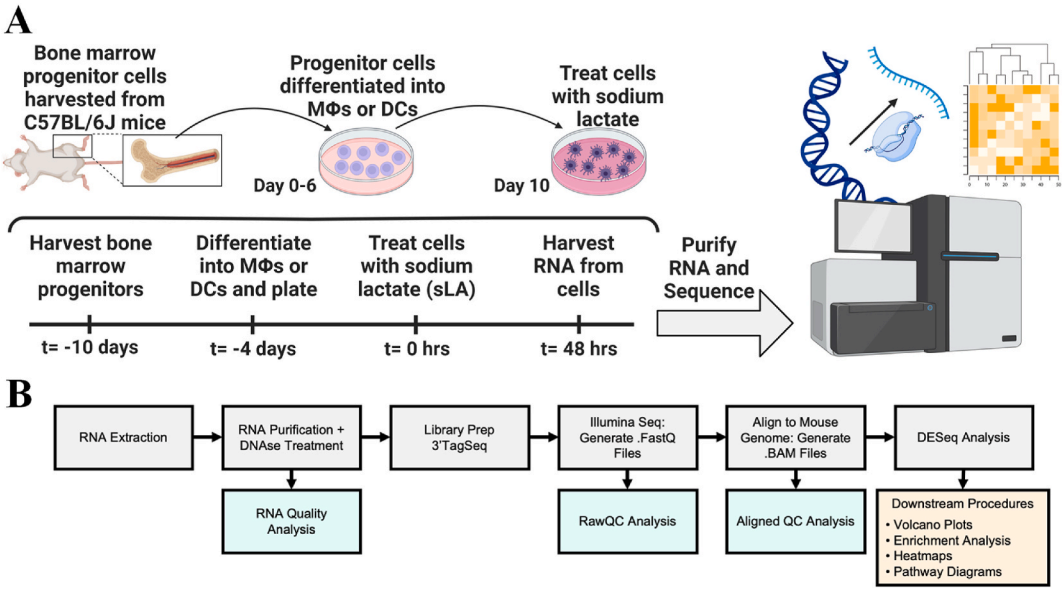

Fig. 1. RNA sequencing and analysis. (**A**) Schematic presentation of the experimental design. Bone marrow progenitor cells were harvested from mice and differentiated into MΦs or DCs over the course of 6 days. On day 10, both cell types were treated with sLA or left untreated as a control. After 48 h, the total RNA in MΦs and DCs was collected, purified and sequenced [39]. (**B**) Overall pipeline of RNA handling and analysis. Following the RNA extraction, the material was purified and RNA quality was assessed. Then, the samples were sequenced and aligned to a mouse genome to generate a differential gene expression output for each treatment comparison [39]. (**C**) Bar graphs showing the significance of gene ontology enrichment terms. Notable pathways were marked with a red asterisk. (**D**) Bar graph displaying the significance of Wikipathway enrichment terms. Notable pathways were marked with a red asterisk.

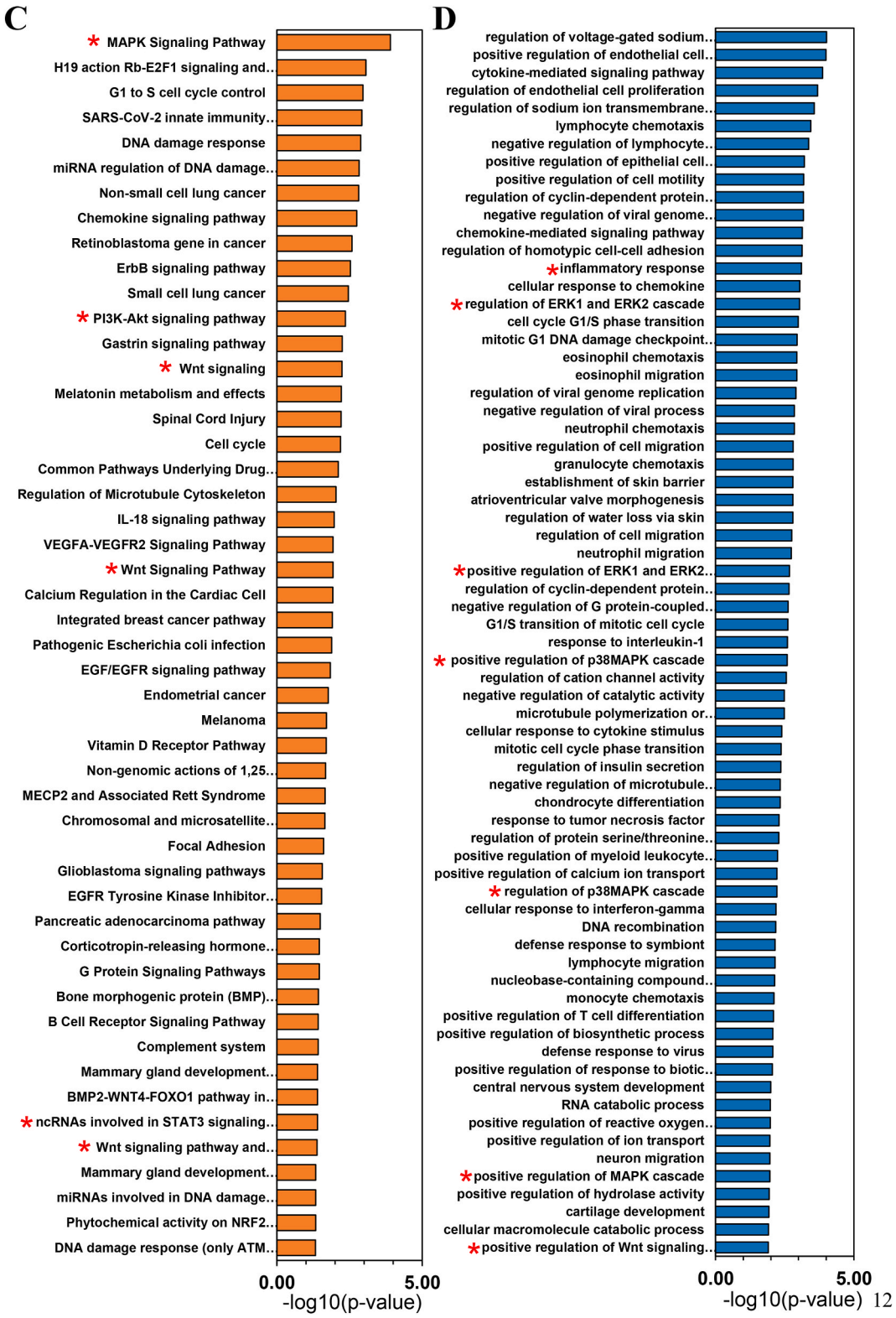

Fig. 1. (*continued*).

temperature. Cells were then incubated at 4 °C overnight with primary antibodies in the blocking buffer: GSK-3β (Ser9, D85E12, CST #5558) diluted at 1:400 ratio, or p-STAT-1 (Tyr701, 58D6, CST #9167) diluted at 1:400 ratio. Cells were then washed twice with PBST, and subsequently stained with a secondary antibody in blocking buffer, Alexa Fluor 647-conjugated anti-rabbit (Life Technologies #A-21245) diluted at 1:500 ratio, followed by Hoechst-33342 (Life Technologies #H3570) diluted at 1:5000 in PBS for

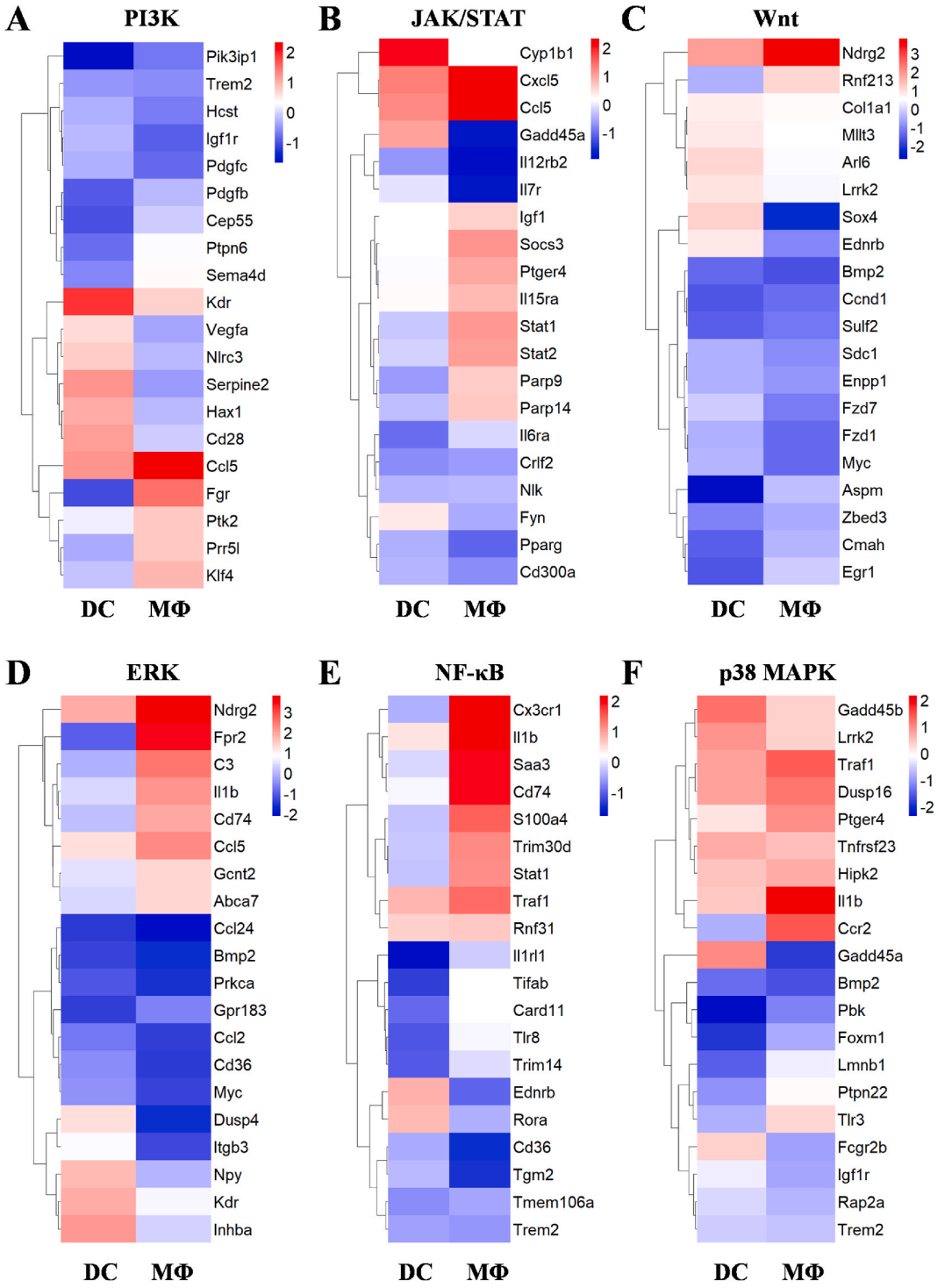

Fig. 2. Heatmap visualization of differentially expressed genes in pathways modulated by sLA treatment in DCs and MΦs. Heatmaps are shown for (**A**) PI3K, (**B**) JAK/STAT, (**C**) Wnt, (**D**) ERK, (**E**) NF-κB, and (**F**) p38 MAPK.

nuclear DNA staining. Plates were then imaged on a Nikon Eclipse Ti inverted microscope (Nikon) with 40X/0.95 NA Plan Apo objective lens, equipped with a Lumencor SOLA or Lumencor SPECTRA X light engine. Fluorescence filters used in the experiment were DAPI (custom ET395/25x - ET460/50 m - T425lpxr, Chroma) and Cy5 (49006, Chroma) filter sets. An image was captured from the center of each well for every replicate under the treatment conditions.

2.8. Image processing and immunofluorescence measurements

Images were processed using custom MATLAB software which identified nuclear and cytosolic compartments [41]. Prior to cell segmentation, background intensity was subtracted from the images. Background intensity was calculated using images taken from an empty well in the 96-well plate. Following appropriate cell segmentation, the images were quantified further for fluorescence intensity. For p-STAT1 measurements, only the average pixel intensity within the nuclear area was included in calculations, whereas for GSK-3β measurements, the average of whole cell pixel intensity was used. Treatment average measurements were then used to calculate fold changes between treatment and control conditions. The fold change method was used to normalize batch effects between replicate experiments.

2.9. Other statistical analysis

Statistical analyses were conducted using a two-tailed one-sample *t*-test to compare the means of each treatment group. A p-value of ≤ 0.05 was considered statistically significant. All analyses were performed using Prism software (Version 8, GraphPad). Data are presented as means ± standard error of the mean (S.E.) from at least three biological replicates.

3. Results

3.1. Gene expression analysis reveals numerous genes and pathways significantly affected by sodium lactate (sLA) treatment

To gain insight into the transcriptional response to sLA in DCs and MΦs, a genome-wide RNA-sequencing study was performed (Fig. 1A–**B**). Here, samples were treated with sLA for 48 h (N = 5 biological replicates per treatment, n = 3 technical replicates). All treated samples used in this study had an RNA Quality Score (RQS) of >7.5 (range 0–10) confirming that all RNA samples had excellent quality and integrity [13].

Following RNA sequencing, sLA exposure in DCs and MΦs exhibited significant gene expression changes as demonstrated in the volcano plots reported previously [39]. The differentially expressed genes were filtered using thresholding of adjusted p-value ≤ 0.05 and $|Log2FC| \geq 0.5$. Then, overlapped genes between DC and MΦ comparison groups isolated 63 significant genes used for enrichment analysis. The significance values of Gene Ontology Biological Process terms and Wikipathway terms for this condensed gene list are shown in Fig. 1C–**D**. The two analyses highlighted some molecular pathways involving general inflammatory cascades associated with immunomodulatory effects of sLA namely, the Janus kinase (JAK)-signal transducer and activator of transcription (STAT), phosphoinositide 3-kinases (PI3Ks), extracellular signal-regulated kinase (ERK), nuclear factor kappa enhancer of activated B cells (NF-κB), p38 mitogen-activated protein kinases (MAPK), and Wnt signaling pathways (Fig. 1–**2**). Further, heatmap visualization of differentially expressed genes in these pathways following sLA treatment in DCs and MΦs is depicted in Fig. 2A–**F**.

3.2. Protein expression analysis hints at pathways that were associated with sLA modulation

The transcriptomic data indicated that JAK/STAT, PI3K, ERK, NF-κB, p38 MAPK, and Wnt pathways were major signaling cascades affected by sLA exposure. As such, we probed these initial findings by quantifying the phosphorylation levels of some critical proteins in these pathways identified by transcriptome analysis. p-STAT1, p-STAT2, p-STAT3, p-JNK, p-PTEN, p-GSK-3β, p-c-Raf, p-PDK1, p-ERK, and p-p38 MAPK were analyzed for the protein level using a Western blot technique (Fig. S2–**3**, **3A**, **3B**, and **3D**). It should be noted that some proteins including p-NF-κB, β-Catenin, and p-Akt were also assayed but not detected due to the antibody sensitivity and protein expression challenges. The detected bands of proteins were analyzed, and the results are depicted in Fig. S2–**3**, **3A**, **3B**, and **3D**. There was a significant increase in the phosphorylation of STAT3, ERK, and p38 MAPK in sLA-treated DCs compared to the untreated control. For sLA-treated MΦs, the phosphorylation levels of STAT1 and STAT2 were significantly increased, while the level of phosphorylated GSK-3β was reduced upon sLA exposure.

3.3. Single cell analyses of the protein signaling molecules identified from the Western blot results are consistent

Further evaluation using flow cytometry and fluorescence imaging was performed to interrogate the effect of sLA on these critical signaling proteins in a single cell manner. Results from flow cytometric analysis corroborated those from the Western blot analysis, demonstrating that sLA promoted the activation of STAT3, ERK, and p38 MAPK pathways in DCs, compared to the control (Fig. 3A and C). Consistency of the protein expression in sLA-treated MΦs was also observed where STAT1 was markedly activated while the level of phosphorylated GSK-3β was reduced relative to the control (Fig. 3A and E). It should be noted that STAT2 phosphorylation was not examined for flow analysis and immunofluorescence imaging due to a lack of commercial availability of the appropriate antibodies. In addition to flow cytometry, immunofluorescence was used to confirm the modulating effect of sLA on these signaling pathways in MΦs. Fluorescence imaging showed that the expression of p-STAT1 and p-GSK-3β was upregulated and downregulated, respectively, in MΦs

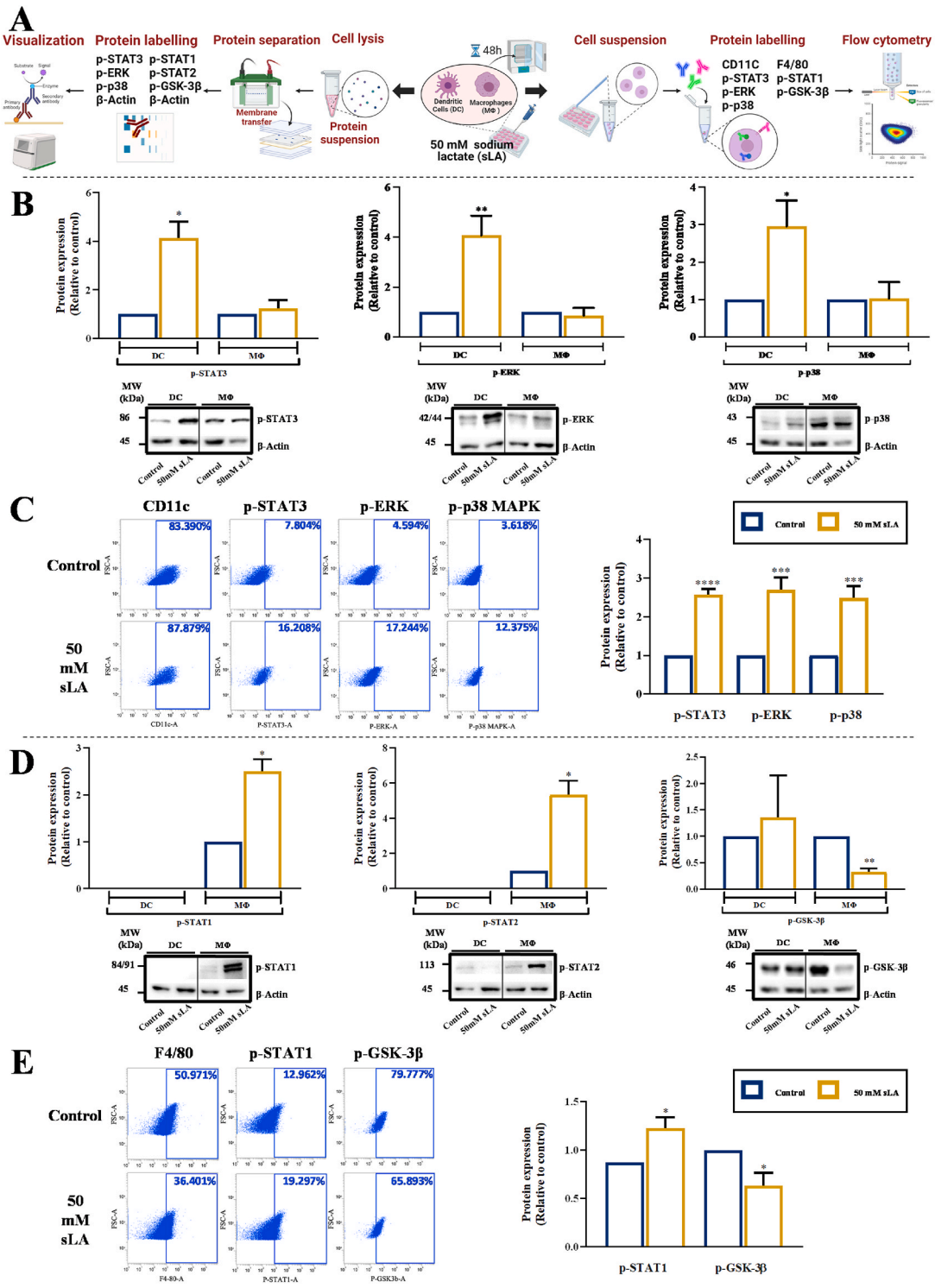

Fig. 3. Effect of sLA on signaling proteins of interest in DCs and MΦs. (**A**) Schematic experiment was depicted. DCs and MΦs were exposed to either 50 mM sLA or control media, and incubated for 48 h. For Western blot analysis, proteins were separated by size and then transferred to the membrane. Protein detection was done using primary antibodies against several proteins including p-STAT3, p-ERK1/2, p-p38 MAPK, p-STAT1, p-STAT2, p-GSK-3β and β-actin. For flow cytometry, DCs cell suspensions were stained with fluorescently tagged anti-CD11c, p-STAT3, p-ERK and p-p38 MAPK. MΦs were stained with fluorescently tagged anti-F4/80, p-STAT1 and p-GSK-3β. The analysis of the phosphorylated protein expression was performed using a flow cytometer. (**B**), (**D**) Western blot results with represented blots showed the effect of sLA on the levels of p-STAT3, p-ERK1/2 and p-p38 MAPK for DCs. For MΦs, p-STAT1, p-STAT2, p-GSK-3β were shown for the effect of sLA. (**C**), (**E**) Flow cytometric assessment

revealed the levels of phosphorylated proteins expression in DCs and MΦs after sLA treatment. The data are demonstrated as the mean ± S.E. from at least three independent experiments, with statistically significant differences calculated by comparing each treatment group to the control. The following symbols indicate the corresponding p-values: *p < 0.05, **p < 0.01, ***p < 0.001, ****p < 0.0001 as determined by a two-tailed one-sample *t*-test.

exposed to sLA (Fig. 4A–**G**). Based on transcriptomic data, pathway mapping diagrams of different notable pathways impacted by sLA treatment in DCs and MΦs are depicted in Fig. 5A–**E**.

4. Discussion

In cancers, the TME has numerous endogenous factors that can mediate the regulation of immune responses [1–4], including lactate. Lactate, a byproduct of elevated glycolytic flux, is one of the pivotal molecules in TME that exerts an immunomodulating effect, seemingly biased towards cancer immune evasion, especially in DCs and MΦs [6–9]. Several studies have demonstrated that DCs and MΦs exposed to LA results in the suppression of pro-inflammatory responses including pro-inflammatory surface markers and cytokines [20–35]. However, the signaling networks influenced by sLA exposure in DCs and MΦs are still not clear. This is a significant knowledge gap not only in malignant tissue but also in mammalian physiology, given the ubiquity of lactate. Moreover, understanding the underlying molecular mechanisms by which sLA fine-tunes antitumor immunity could be instrumental for the rational design of therapeutic agents against cancers.

Generally, the phosphorylation of proteins is the key post translational modification essential for cell signal transduction [42]. In most cases, phosphorylation involves an activation of proteins in signaling cascades for example, STAT and MAPK pathways [43–48]. The STAT pathways are broadly involved in the perturbation in immune function, including infection, immune tolerance, barrier function, and cancer prevention [43–45]. A previous study showed that STAT3 signaling was linked to the induction of a tolerogenic immune response due to its role in the downregulation of costimulatory molecules [49]. Interestingly, even in an inflammatory environment, STAT3 regulated stable tolerogenic properties of DCs [50]. STAT3-deficient DCs demonstrated enhanced immune activity as indicated by an increase in cytokine production and T-cell activation [51], underscoring the importance of STAT3 on DC activation. In our study, we showed that p-STAT3 was upregulated in DCs exposed to sLA, which may impair DC maturation and result in reduced capacity to prime T cells. STAT1 and STAT2 have different roles in immunity—they are critical components in interferon (IFN) signaling, which regulates the host response during pathogen infection [52–61]. A study by Gopal et al. shed some light on the role of STAT2 during influenza and bacterial infection [55]. In influenza-infected *Stat2*−/− mice, there was an increase in levels of the inflammatory cytokines, and an increase in levels of the Type 2 cytokines (IL-4 and IL-5) [55]. Interestingly, the BMMΦs in *Stat2*−/− mice elicited both M1 and M2 macrophage phenotypes based on the gene and surface antigen expression during infection [55]. Here, we observed an upregulation of p-STAT1 and p-STAT2 in MΦs exposed to sLA. Inferentially, this may lead to impaired macrophage differentiation and downstream immune activation. Collectively, STAT signaling pathways are adversely affected by sLA in both DCs and MΦs, providing insight on imbalances in regulation of cancer-associated immune activity.

Apart from the STAT signaling pathway, MAPK pathway has been shown to tightly regulate both pro- and anti-inflammatory immune responses [46–48]. The main MAPK sub-families comprise p38 MAPK, JNK, and ERK, which play a pivotal role in the innate immune responses through the three-module phosphorylation cascade acting on specific serine and threonine amino acid residues of protein kinases [46–48]. Specific to innate immunity, previous studies suggested that the maturation of human monocyte-derived DCs (MODCs) was regulated through the MAPK signaling pathway [46,62,63]. In the maturation process of MODCs, upregulation of key stimulatory molecules namely CD40, CD80, CD83, CD86, and MHC class II molecules is pivotal for downstream stimulation of naïve T cells in the primary immune response [46,62,63]. During maturation, MODCs also secreted several cytokines including IL-12 p70 to facilitate immune activity [46,62,63]. p38 MAPK and ERK are the two subfamilies of the MAPK pathway that have been intensively studied due to the availability of specific inhibitors [46,62,63]. The inhibition of p38 MAPK caused a drastic reduction in the surface expression of CD40, CD80, CD86, HLA-DR, and CD83 induced by LPS in immature MODCs and also inhibited the production of IL-12 p40 and IL-12 p70 [46,62,63]. The allostimulatory capacity of MODCs activated by LPS was also decreased by a p38 MAPK inhibitor [46,62,63]. Overall, the p38 MAPK signaling pathway activated the expression of key stimulatory surface molecules, cytokine production, and allostimulatory functions of the DCs [46,62–64]. The conclusions on ERK inhibition in stimulated DCs are less clear [65,66]. In some instances, ERK inhibition did not hinder the upregulation of CD80, CD86, CD83, HLA-DR, or CD40 during LPS or TNF-α challenge in MODCs [65,66]. Meanwhile, a slight increase in the surface expression of CD83, CD86, or MHC class II was mediated by ERK inhibition during DC maturation induced by stimuli such as UVB or $NiCl_2$ [57,65,66]. Similar to p38 MAPK inhibition, the inhibition of ERK dampened the production of pro-inflammatory cytokines (TNF-α, IL-1β, IL-6, or IL-8) induced by LPS or $NiCl_2$ [46,63,65,66]. On the other hand, the inhibition of ERK increased the productions of IL-12 p40 and IL-12 p70 in response to LPS or TNF-α [46,65,67,68]. Depending on the maturation stimuli, ERK inhibition either had no effect or induced an allostimulatory phenotype of MODCs [46,63,65–68]. Taken together, the production of cytokines and the expression of co-stimulatory molecules during maturation in MODCs are profoundly complex and rather differentially regulated through different subfamilies of the MAPK signaling pathways [46,63,65–68]. Here, we demonstrated that sLA exposure increased the phosphorylation of p38 MAPK and ERK in immature DCs. The change in the phosphorylation of the two key MAPK proteins in the immature DCs due to the presence of sLA may cause an imbalance in this important biochemical network, and further, dysregulated immunosurveillance by DCs in cancerous tissue.

Tumor cell-intrinsic Wnt signaling plays a key role in the evasion of antitumor immunity in several human cancers [69–71]. One of the prominent routes in mediating the Wnt signaling pathway is via the activity of glycogen synthase kinase-3 (GSK-3) [72]. GSK-3

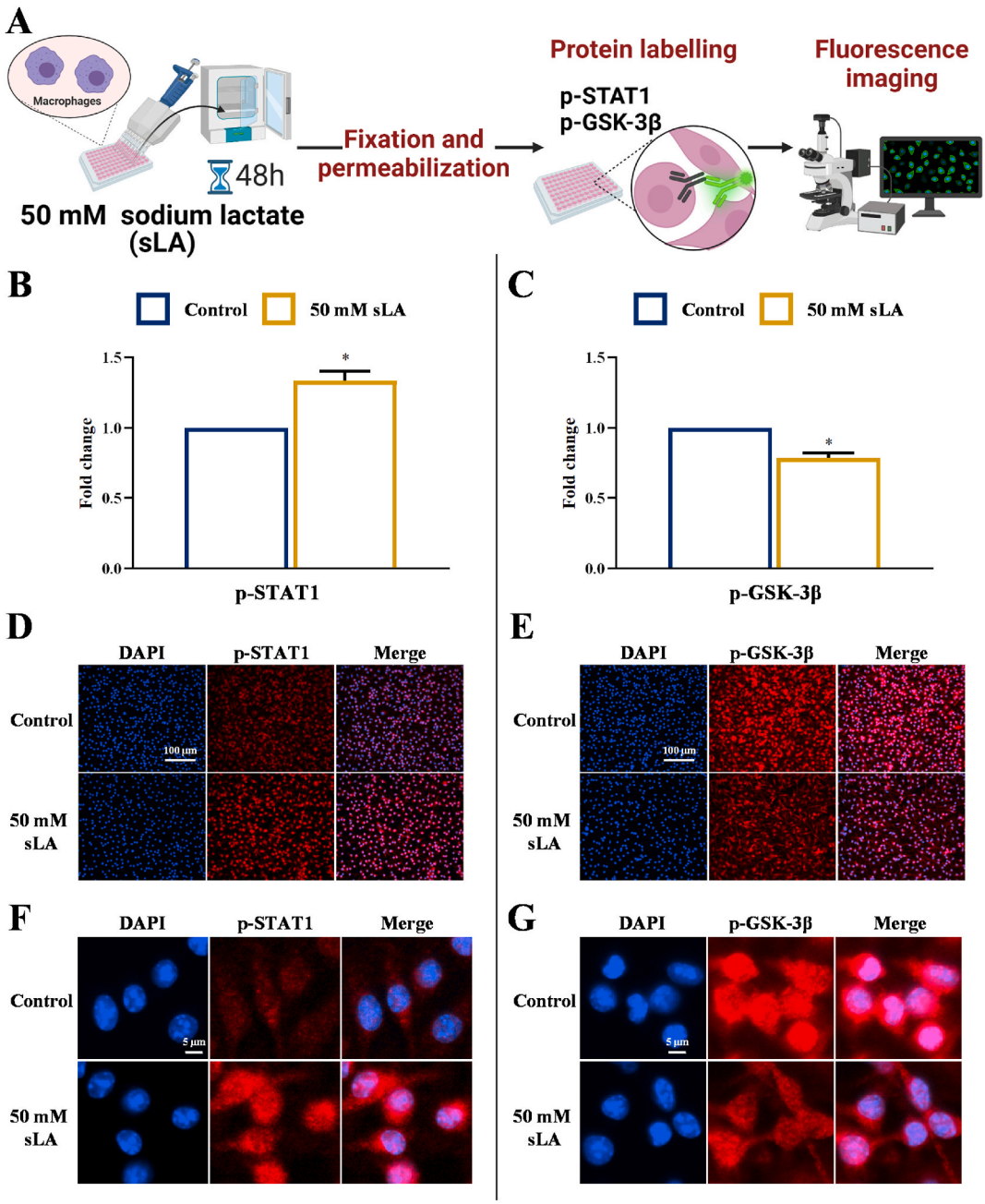

Fig. 4. Immunofluorescence was performed to further confirm the effect of sLA on the signaling proteins of interest in MΦs. (**A**) Schematic experiment was depicted. MΦs were exposed to either 50 mM sLA or control media, and incubated for 48 h. Cells were washed with PBS, then fixed and permeabilized and blocked. Subsequently, cells were incubated with primary antibodies against p-GSK-3β or p-STAT1. The plates were imaged using a fluorescence microscope equipped with a 40X objective lens, capturing both (**D**), (**E**) standard and (**F**), (**G**) zoomed-in views. (**B**), (**D**), (**F**) Immunofluorescence results with represented images revealed the levels of phosphorylated proteins: p-STAT1 in MΦs after sLA treatment. (**C**), (**E**), (**G**) Immunofluorescence results with represented images revealed the levels of phosphorylated proteins: p-GSK-3β in MΦs after sLA treatment. The data are demonstrated as the mean ± S.E. from at least three independent experiments, with statistically significant differences calculated by comparing each treatment group to the control. The following symbols indicate the corresponding p-values: *$p < 0.05$ as determined by a two-tailed one-sample *t*-test.

comprises two isoforms, GSK-3α and GSK-3β, which have been closely associated with inflammation [72]. GSK-3 regulates multiple immune cells, including MΦs, T cells, and DCs by influencing their viability, proliferation, differentiation, migration, and macrophage phenotype. GSK-3 activity is regulated by phosphorylation at certain locations [72]. Phosphorylation at tyrosine (Tyr) residue 279 and Tyr 216 promotes activation, while that at serine (Ser) residue 21 and Ser 9 lead to the inhibition of GSK-3α and GSK-3β activities,

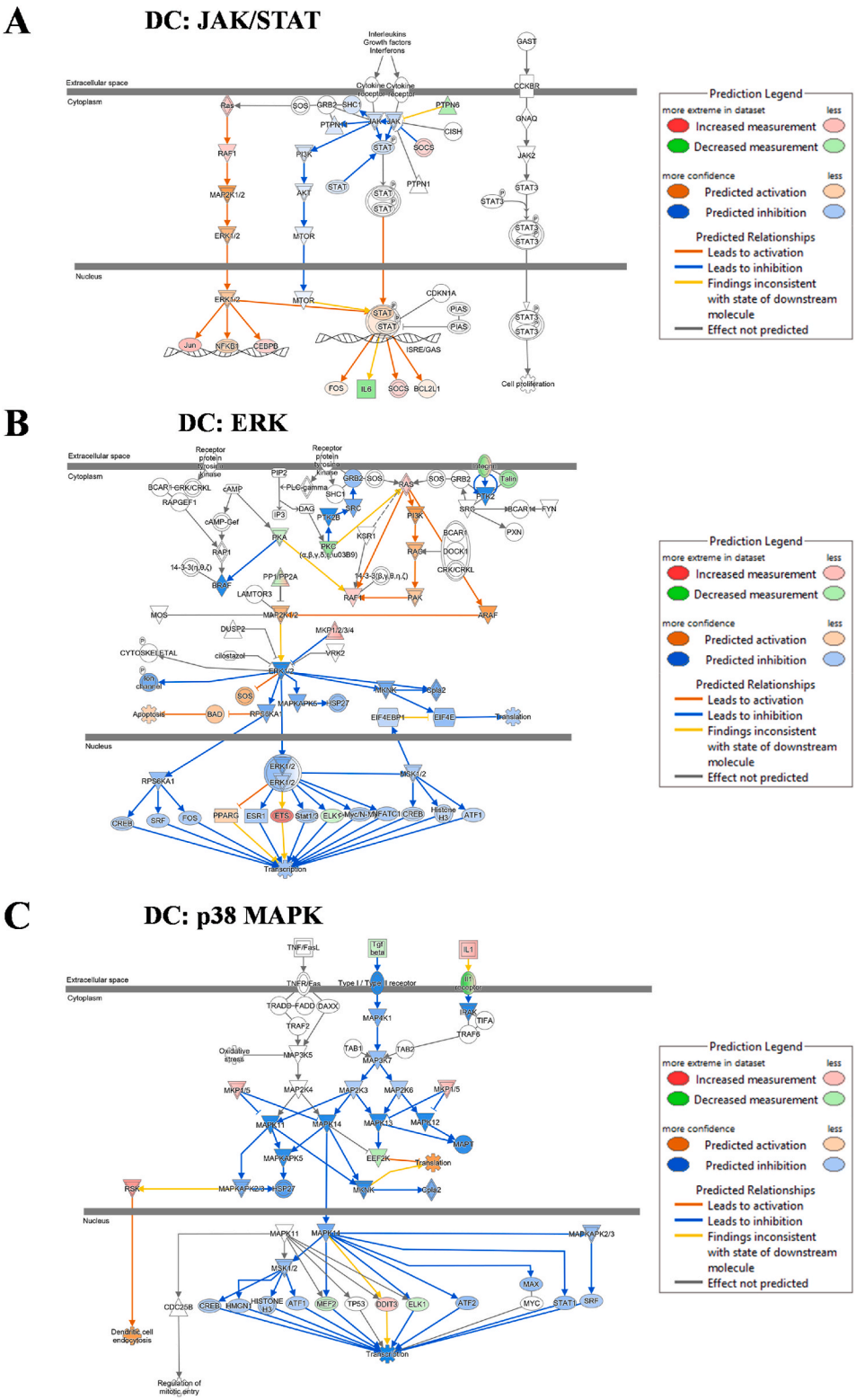

Fig. 5. Pathway mapping diagrams of different notable pathways aberrantly modulated by sLA treatment in DCs and MΦs. For DCs, pathway diagrams are shown for (**A**) JAK/STAT, (**B**) ERK, and (**C**) p38 MAPK. For MΦs, pathway diagrams are shown for (**D**) JAK/STAT and (**E**) Wnt. Parameters including changes in the expression and predicted activation/inhibition states are displayed by color shading.

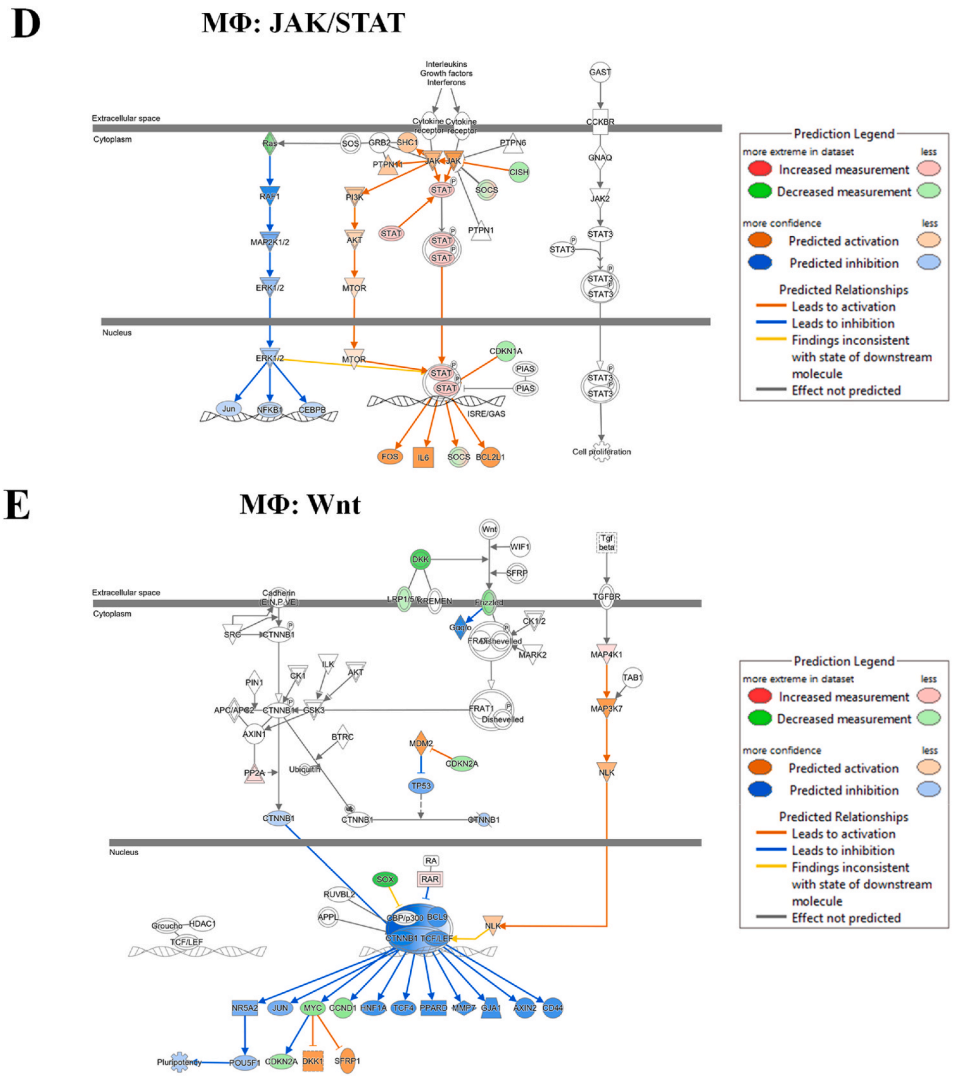

Fig. 5. (*continued*).

respectively [72]. Even though several studies have reported a relationship between immune activity, Wnt signaling pathway, and phosphorylation of GSK-3, the results are still controversial [72]. It has been reported that GSK-3 mediates inflammatory responses (tumor necrosis factor-α, IL-1β, IL6, and IL12 production) in human monocytes. Further, application of GSK-3 inhibitors provided an anti-inflammatory response, which led to beneficial effect in models of multiple inflammatory diseases including arthritis, colitis, diabetes, and atherosclerosis [72–74]. Our result showed that sLA exposure significantly decreased the phosphorylation on Ser 9 of GSK-3β. The modulatory effect of sLA on the activity of GSK-3β might have downstream impacts on the global biochemical signaling that regulates immunophenotypes of MΦs.

Previously, we investigated the immunogenic effect of sLA on DCs and MΦs during immature stage (without LPS challenge). DCs exposed to a biologically-relevant concentration of sLA in TME (50 mM) for 48 h marginally demonstrated no significant differences in surface expressions of CD80, CD86, MHC class II, compared to untreated DCs [39]. However, the exposure of DCs to sLA down-regulated the expression of CCR7, a molecule associated with the mobilization of innate immune cells [39]. In addition, we observed that sLA-treated DCs were ineffective in stimulating allogenic T cells, as demonstrated by the allogeneic mixed lymphocyte reaction [39]. Interestingly, LPS-challenged DCs pretreated with sLA reduced the production and secretion of IL-12 p70 [39]. The results presented herein help to fill the knowledge gap in the previous study by providing insight into key signaling protein molecules mediated by sLA. For instance, based on our observations (and other published literature), we can infer that the phosphorylation of STAT3, due to lactate exposure, may contribute to the downregulation of CCR7 expression and allostimulatory capacity, further substantiating previously reported findings [49–51]. Moreover, sLA exposure may compromise DC activation through the dysregulation of p-STAT3 and p-ERK, which can downregulate IL-12 p70 secretion [39]. With respect to MΦs, we previously showed that sLA-exposed MΦs were polarized toward pro-tumor, M2-like phenotype as evidence by the downregulation of CD38 (anti-tumoral

marker, M1) and upregulation of CD163 and Arg1 (pro-tumor markers) [39]. Surprisingly, MΦs preserved their ability to stimulate T cells despite exposure to sLA. In addition, MΦs after sLA exposure had little effect on CCR7 expression [39]. In the present study, MΦs had altered phosphorylation of STAT1, STAT2 and GSK-3β after sLA treatment. Collectively, the imbalance in these three signaling molecules may result in aberrant polarization of MΦs [39]. However, more comprehensive studies using phosphoproteomic analysis, specific inhibitors or gene editing approaches are required to fully understand the mechanisms involved in cancer-mediated immunomodulation, especially regarding a high lactate level in the TME. Critically, this study only considers a single time window following lactate exposure. However, these signaling cascades are dynamic and have varying states and effects with respect to time after exposure to a modulating molecule. It is critical that future studies capture the full temporal picture of lactate modulation of immune cells. Nevertheless, this study will serve as a guide for which signaling networks should be probed in the future.

5. Conclusions

Altogether, this study revealed key signaling pathways significantly impacted by sLA exposure in two key players of anticancer immunity—DCs and MΦs. Lactate exposure in bone marrow-derived DCs significantly disrupted STAT3, ERK, and p38 MAPK signaling cascades, while in bone marrow-derived-MΦs, immunomodulating effects of sLA are more pronounced in the STAT1, STAT2 and GSK-3β signaling pathways. These results were corroborated via multiple assays including RNA sequencing and flow cytometry. Importantly, this knowledge may serve as a basis for further optimizing cancer immunotherapy through the inhibition of key signaling pathways modulated by lactate, a major metabolic by-product in the tumor microenvironment.

CRediT authorship contribution statement

Rapeepat Sangsuwan: Writing – review & editing, Writing – original draft, Visualization, Validation, Supervision, Project administration, Methodology, Investigation, Formal analysis, Data curation. **Bhasirie Thuamsang:** Writing – original draft, Visualization, Methodology, Investigation, Formal analysis, Data curation. **Noah Pacifici:** Writing – review & editing, Writing – original draft, Visualization, Validation, Software, Methodology, Investigation, Formal analysis, Data curation. **Phum Tachachartvanich:** Writing – review & editing, Writing – original draft, Data curation. **Devan Murphy:** Methodology, Investigation, Formal analysis, Data curation. **Abhineet Ram:** Methodology, Investigation, Formal analysis, Data curation. **John Albeck:** Supervision, Project administration, Investigation. **Jamal S. Lewis:** Writing – review & editing, Supervision, Resources, Project administration, Funding acquisition, Formal analysis, Data curation, Conceptualization.

Ethics statement

All animals were housed in a specific pathogen-free environment in the University of California, Davis facilities and used following the detailed experimental protocol (#21139) approved by the University of California Institutional Animal Care and Use Committee (IACUC).

Data availability statement

Transcriptomic data have been deposited at Dryad and is publicly available for download via the following link: https://datadryad.org/stash/dataset/doi:10.5061/dryad.bzkh189kq.

Funding

We acknowledge support from the National Institutes of Health NIAID grant - R01AI139399 which was awarded to J.S.L. We also acknowledge the support from the National Research Council of Thailand (NRCT) and Chulabhorn Research Institute (Grant No. N42A660434 and N42A660435) to R.S. and P.T.

Declaration of competing interest

The authors declare that they have no known competing financial interests or personal relationships that could have appeared to influence the work reported in this paper.

Acknowledgments

There are no specific acknowledgements on this body of work.

Appendix A. Supplementary data

Supplementary data to this article can be found online at https://doi.org/10.1016/j.heliyon.2025.e42098.

References

[1] D.G. DeNardo, B. Ruffell, Macrophages as regulators of tumour immunity and immunotherapy, Nat. Rev. Immunol. 19 (2019) 369–382.
[2] A.E. Marciscano, N. Anandasabapathy, The role of dendritic cells in cancer and anti-tumor immunity. Seminars in Immunology, Elsevier, 2021 101481.
[3] A. Gardner, B. Ruffell, Dendritic cells and cancer immunity, Trends Immunol. 37 (2016) 855–865.
[4] O. Demaria, S. Cornen, M. Daëron, Y. Morel, R. Medzhitov, E. Vivier, Harnessing innate immunity in cancer therapy, Nature 574 (2019) 45–56.
[5] M. Certo, C.-H. Tsai, V. Pucino, P.-C. Ho, C. Mauro, Lactate modulation of immune responses in inflammatory versus tumour microenvironments, Nat. Rev. Immunol. 21 (2021) 151–161.
[6] O. Warburg, On respiratory impairment in cancer cells, Science 124 (1956) 269–270.
[7] W.H. Koppenol, P.L. Bounds, C.V. Dang, Otto Warburg's contributions to current concepts of cancer metabolism, Nat. Rev. Cancer 11 (2011) 325–337.
[8] J.-w. Kim, I. Tchernyshyov, G.L. Semenza, C.V. Dang, HIF-1-mediated expression of pyruvate dehydrogenase kinase: a metabolic switch required for cellular adaptation to hypoxia, Cell Metabol. 3 (2006) 177–185.
[9] I. Papandreou, R.A. Cairns, L. Fontana, A.L. Lim, N.C. Denko, HIF-1 mediates adaptation to hypoxia by actively downregulating mitochondrial oxygen consumption, Cell Metabol. 3 (2006) 187–197.
[10] R. Shiratori, K. Furuichi, M. Yamaguchi, N. Miyazaki, H. Aoki, H. Chibana, K. Ito, S. Aoki, Glycolytic suppression dramatically changes the intracellular metabolic profile of multiple cancer cell lines in a mitochondrial metabolism-dependent manner, Sci. Rep. 9 (2019) 1–15.
[11] K.G. de la Cruz-López, L.J. Castro-Muñoz, D.O. Reyes-Hernández, A. García-Carrancá, J. Manzo-Merino, Lactate in the regulation of tumor microenvironment and therapeutic approaches, Front. Oncol. 9 (2019) 1143.
[12] S. Walenta, M. Wetterling, M. Lehrke, G. Schwickert, K. Sundfør, E.K. Rofstad, W. Mueller-Klieser, High lactate levels predict likelihood of metastases, tumor recurrence, and restricted patient survival in human cervical cancers, Cancer Res. 60 (2000) 916–921.
[13] S. Walenta, A. Salameh, H. Lyng, J.F. Evensen, M. Mitze, E.K. Rofstad, W. Mueller-Klieser, Correlation of high lactate levels in head and neck tumors with incidence of metastasis, Am. J. Pathol. 150 (1997) 409.
[14] D.M. Brizel, T. Schroeder, R.L. Scher, S. Walenta, R.W. Clough, M.W. Dewhirst, W. Mueller-Klieser, Elevated tumor lactate concentrations predict for an increased risk of metastases in head-and-neck cancer, Int. J. Radiat. Oncol. Biol. Phys. 51 (2001) 349–353.
[15] S. Indraccolo, W. Mueller-Klieser, Potential of induced metabolic bioluminescence imaging to uncover metabolic effects of antiangiogenic therapy in tumors, Front. Oncol. 6 (2016) 15.
[16] A. Naik, J. Decock, Lactate metabolism and immune modulation in breast cancer: a focused review on triple negative breast tumors, Front. Oncol. 10 (2020) 598626.
[17] S.K. Parks, W. Mueller-Klieser, J. Pouysségur, Lactate and acidity in the cancer microenvironment, Annu. Rev. Cell Biol. 4 (2020) 141–158.
[18] R.P. Allen, A. Bolandparvaz, J.A. Ma, V.A. Manickam, J.S. Lewis, Latent, immunosuppressive nature of poly (lactic-co-glycolic acid) microparticles, ACS Biomater. Sci. Eng. 4 (2018) 900–918.
[19] E. Gottfried, L.A. Kunz-Schughart, S. Ebner, W. Mueller-Klieser, S. Hoves, R. Andreesen, A. Mackensen, M. Kreutz, Tumor-derived lactic acid modulates dendritic cell activation and antigen expression, Blood 107 (2006) 2013–2021.
[20] A. Nasi, T. Fekete, A. Krishnamurthy, S. Snowden, E. Rajnavölgyi, A.I. Catrina, C.E. Wheelock, N. Vivar, B. Rethi, Dendritic cell reprogramming by endogenously produced lactic acid, J. Immunol. 191 (2013) 3090–3099.
[21] D. Raychaudhuri, R. Bhattacharya, B.P. Sinha, C.S.C. Liu, A.R. Ghosh, O. Rahaman, P. Bandopadhyay, J. Sarif, R. D'Rozario, S. Paul, Lactate induces pro-tumor reprogramming in intratumoral plasmacytoid dendritic cells, Front. Immunol. 10 (2019) 1878.
[22] T.P. Brown, P. Bhattacharjee, S. Ramachandran, S. Sivaprakasam, B. Ristic, M.O.F. Sikder, V. Ganapathy, The lactate receptor GPR81 promotes breast cancer growth via a paracrine mechanism involving antigen-presenting cells in the tumor microenvironment, Oncogene 39 (2020) 3292–3304.
[23] N. Caronni, F. Simoncello, F. Stafetta, C. Guarnaccia, J.S. Ruiz-Moreno, B. Opitz, T. Galli, V. Proux-Gillardeaux, F. Benvenuti, Downregulation of membrane trafficking proteins and lactate conditioning determine loss of dendritic cell function in lung CancerMechanisms of DC suppression in lung tumors, Cancer Res. 78 (2018) 1685–1699.
[24] O.R. Colegio, N.-Q. Chu, A.L. Szabo, T. Chu, A.M. Rhebergen, V. Jairam, N. Cyrus, C.E. Brokowski, S.C. Eisenbarth, G.M. Phillips, Functional polarization of tumour-associated macrophages by tumour-derived lactic acid, Nature 513 (2014) 559–563.
[25] A. Errea, D. Cayet, P. Marchetti, C. Tang, J. Kluza, S. Offermanns, J.-C. Sirard, M. Rumbo, Lactate inhibits the pro-inflammatory response and metabolic reprogramming in murine macrophages in a GPR81-independent manner, PLoS One 11 (2016) e0163694.
[26] P. Chen, H. Zuo, H. Xiong, M.J. Kolar, Q. Chu, A. Saghatelian, D.J. Siegwart, Y. Wan, Gpr132 Sensing of Lactate Mediates Tumor–Macrophage Interplay to Promote Breast Cancer Metastasis, vol. 114, Proceedings of the National Academy of Sciences, 2017, pp. 580–585.
[27] T. Ohashi, M. Aoki, H. Tomita, T. Akazawa, K. Sato, B. Kuze, K. Mizuta, A. Hara, H. Nagaoka, N. Inoue, M2-like macrophage polarization in high lactic acid-producing head and neck cancer, Cancer Sci. 108 (2017) 1128–1134.
[28] J. Yang, J. Yan, B. Liu, Targeting VEGF/VEGFR to modulate antitumor immunity, Front. Immunol. 9 (2018) 978.
[29] S.C. Stone, R.A.M. Rossetti, K.L.F. Alvarez, J.P. Carvalho, P.F.R. Margarido, E.C. Baracat, M. Tacla, E. Boccardo, K. Yokochi, N.P. Lorenzi, Lactate secreted by cervical cancer cells modulates macrophage phenotype, J. Leukoc. Biol. 105 (2019) 1041–1054.
[30] H. Ye, Q. Zhou, S. Zheng, G. Li, Q. Lin, L. Wei, Z. Fu, B. Zhang, Y. Liu, Z. Li, Tumor-associated macrophages promote progression and the Warburg effect via CCL18/NF-kB/VCAM-1 pathway in pancreatic ductal adenocarcinoma, Cell Death Dis. 9 (2018) 453.
[31] X. Mu, W. Shi, Y. Xu, C. Xu, T. Zhao, B. Geng, J. Yang, J. Pan, S. Hu, C. Zhang, Tumor-derived lactate induces M2 macrophage polarization via the activation of the ERK/STAT3 signaling pathway in breast cancer, Cell Cycle 17 (2018) 428–438.
[32] A. Brand, K. Singer, G.E. Koehl, M. Kolitzus, G. Schoenhammer, A. Thiel, C. Matos, C. Bruss, S. Klobuch, K. Peter, LDHA-associated lactic acid production blunts tumor immunosurveillance by T and NK cells, Cell Metabol. 24 (2016) 657–671.
[33] P. Ranganathan, A. Shanmugam, D. Swafford, A. Suryawanshi, P. Bhattacharjee, M.S. Hussein, P.A. Koni, P.D. Prasad, Z.B. Kurago, M. Thangaraju, GPR81, a cell-surface receptor for lactate, regulates intestinal homeostasis and protects mice from experimental colitis, J. Immunol. 200 (2018) 1781–1789.
[34] Z. Husain, Y. Huang, P. Seth, V.P. Sukhatme, Tumor-derived lactate modifies antitumor immune response: effect on myeloid-derived suppressor cells and NK cells, J. Immunol. 191 (2013) 1486–1495.
[35] Y. Long, Z. Gao, X. Hu, F. Xiang, Z. Wu, J. Zhang, X. Han, L. Yin, J. Qin, L. Lan, Downregulation of MCT 4 for lactate exchange promotes the cytotoxicity of NK cells in breast carcinoma, Cancer Med. 7 (2018) 4690–4700.
[36] M. Vermeulen, M. Giordano, A.S. Trevani, C. Sedlik, R. Gamberale, P. Fernández-Calotti, G. Salamone, S. Raiden, J. Sanjurjo, J.R. Geffner, Acidosis improves uptake of antigens and MHC class I-restricted presentation by dendritic cells, J. Immunol. 172 (2004) 3196–3204.
[37] T. Bohn, S. Rapp, N. Luther, M. Klein, T.-J. Bruehl, N. Kojima, P. Aranda Lopez, J. Hahlbrock, S. Muth, S. Endo, Tumor immunoevasion via acidosis-dependent induction of regulatory tumor-associated macrophages, Nat. Immunol. 19 (2018) 1319–1329.
[38] F.M. Marim, T.N. Silveira, D.S. Lima Jr., D.S. Zamboni, A method for generation of bone marrow-derived macrophages from cryopreserved mouse bone marrow cells, PLoS One 5 (2010) e15263.
[39] R. Sangsuwan, B. Thuamsang, N. Pacifici, R. Allen, H. Han, S. Miakicheva, J.S. Lewis, Lactate exposure promotes immunosuppressive phenotypes in innate immune cells, Cell. Mol. Bioeng. 13 (2020) 541–557.
[40] R. Sangsuwan, A.C. Obermeyer, P. Tachachartvanich, K.K. Palaniappan, M.B. Francis, Direct detection of nitrotyrosine-containing proteins using an aniline-based oxidative coupling strategy, Chem. Commun. 52 (2016) 10036–10039.
[41] M. Pargett, T.E. Gillies, C.K. Teragawa, B. Sparta, J.G. Albeck, Single-cell imaging of ERK signaling using fluorescent biosensors, Kinase Signaling Networks (2017) 35–59.
[42] K. Pang, W. Wang, J.X. Qin, Z.D. Shi, L. Hao, Y.Y. Ma, H. Xu, Z.X. Wu, D. Pan, Z.S. Chen, Role of protein phosphorylation in cell signaling, disease, and the intervention therapy, MedComm 3 (2022) e175.

[43] Q. Hu, Q. Bian, D. Rong, L. Wang, J. Song, H.-S. Huang, J. Zeng, J. Mei, P.-Y. Wang, JAK/STAT pathway: extracellular signals, diseases, immunity, and therapeutic regimens, Front. Bioeng. Biotechnol. 11 (2023) 1110765.
[44] K. Shuai, B. Liu, Regulation of JAK–STAT signalling in the immune system, Nat. Rev. Immunol. 3 (2003) 900–911.
[45] A.V. Villarino, Y. Kanno, J.R. Ferdinand, J.J. O'Shea, Mechanisms of Jak/STAT signaling in immunity and disease, J. Immunol. 194 (2015) 21–27.
[46] T. Nakahara, Y. Moroi, H. Uchi, M. Furue, Differential role of MAPK signaling in human dendritic cell maturation and Th1/Th2 engagement, J. Dermatol. Sci. 42 (2006) 1–11.
[47] L. Chang, M. Karin, Mammalian MAP kinase signalling cascades, Nature 410 (2001) 37–40.
[48] G.L. Johnson, R. Lapadat, Mitogen-activated protein kinase pathways mediated by ERK, JNK, and p38 protein kinases, Science. 298 (2002) 1911–1912.
[49] Y. Nefedova, P. Cheng, D. Gilkes, M. Blaskovich, A.A. Beg, S.M. Sebti, D.I. Gabrilovich, Activation of dendritic cells via inhibition of Jak2/STAT3 signaling, J. Immunol. 175 (2005) 4338–4346.
[50] K. Dáňová, A. Klapetková, J. Kayserová, A. Šedivá, R. Špíšek, L.P. Jelínková, NF-κB, p38 MAPK, ERK1/2, mTOR, STAT3 and increased glycolysis regulate stability of paricalcitol/dexamethasone-generated tolerogenic dendritic cells in the inflammatory environment, Oncotarget 6 (2015) 14123.
[51] J.A. Melillo, L. Song, G. Bhagat, A.B. Blazquez, C.R. Plumlee, C. Lee, C. Berin, B. Reizis, C. Schindler, Dendritic cell (DC)-specific targeting reveals Stat3 as a negative regulator of DC function, J. Immunol. 184 (2010) 2638–2645.
[52] E.M. Coccia, N.D. Russo, E. Stellacci, U. Testa, G. Marziali, A. Battistini, STAT1 activation during monocyte to macrophage maturation: role of adhesion molecules, Int. Immunol. 11 (1999) 1075–1083.
[53] P. Kovarik, D. Stoiber, M. Novy, T. Decker, Stat1 combines signals derived from IFN-γ and LPS receptors during macrophage activation, EMBO J. 17 (1998) 3660–3668.
[54] W. Alazawi, H. Heath, J.A. Waters, A. Woodfin, A.J. O'Brien, A.J. Scarzello, B. Ma, Y. Lopez-Otalora, M. Jacobs, G. Petts, Stat2 loss leads to cytokine-independent, cell-mediated lethality in LPS-induced sepsis, Proc. Natl. Acad. Sci. USA 110 (2013) 8656–8661.
[55] R. Gopal, B. Lee, K.J. McHugh, H.E. Rich, K. Ramanan, S. Mandalapu, M.E. Clay, M.L. Manni, K.M. Robinson, J. Rangel-Moreno, STAT2-mediated regulation of macrophage phenotype during influenza and bacterial super-infection, J. Immunol. 198 (2017), 153.115-153.115.
[56] R. Gopal, B. Lee, K.J. McHugh, H.E. Rich, K. Ramanan, S. Mandalapu, M.E. Clay, P.J. Seger, R.I. Enelow, M.L. Manni, STAT2 signaling regulates macrophage phenotype during influenza and bacterial super-infection, Front. Immunol. 9 (2018) 2151.
[57] S. Kemmner, Q. Bachmann, S. Steiger, G. Lorenz, M. Honarpisheh, O. Foresto-Neto, S. Wang, J. Carbajo-Lozoya, V. Alt, C. Schulte, STAT1 regulates macrophage number and phenotype and prevents renal fibrosis after ischemia-reperfusion injury, Am. J. Physiol. Ren. Physiol. 316 (2019) F277–F291.
[58] X. Li, S. Liu, K.R. Rai, W. Zhou, S. Wang, X. Chi, G. Guo, J.-L. Chen, S. Liu, Initial activation of STAT2 induced by IAV infection is critical for innate antiviral immunity, Front. Immunol. 13 (2022) 960544.
[59] T. Liang, J. Chen, G. Xu, Z. Zhang, J. Xue, H. Zeng, J. Jiang, T. Chen, Z. Qin, H. Li, STAT1 and CXCL10 involve in M1 macrophage polarization that may affect osteolysis and bone remodeling in extrapulmonary tuberculosis, Gene 809 (2022) 146040.
[60] B. Lee, R. Gopal, M.L. Manni, K.J. McHugh, S. Mandalapu, K.M. Robinson, J.F. Alcorn, STAT1 Is required for suppression of type 17 immunity during influenza and bacterial superinfection, ImmunoHorizons 1 (2017) 81–91.
[61] Y. Xiong, Y. Li, X. Cui, L. Zhang, X. Yang, H. Liu, ADAP restraint of STAT1 signaling regulates macrophage phagocytosis in immune thrombocytopenia, Cell. Mol. Immunol. 19 (2022) 898–912.
[62] J.-F.o. Arrighi, M. Rebsamen, F.o. Rousset, V. Kindler, C. Hauser, A critical role for p38 mitogen-activated protein kinase in the maturation of human blood-derived dendritic cells induced by lipopolysaccharide, TNF-α, and contact sensitizers, J. Immunol. 166 (2001) 3837–3845.
[63] T. Nakahara, H. Uchi, K. Urabe, Q. Chen, M. Furue, Y. Moroi, Role of c-Jun N-terminal kinase on lipopolysaccharide induced maturation of human monocyte-derived dendritic cells, Int. Immunol. 16 (2004) 1701–1709.
[64] Y. Lu, M. Zhang, S. Wang, B. Hong, Z. Wang, H. Li, Y. Zheng, J. Yang, R.E. Davis, J. Qian, p38 MAPK-inhibited dendritic cells induce superior antitumour immune responses and overcome regulatory T-cell-mediated immunosuppression, Nat. Commun. 5 (2014) 4229.
[65] S. Aiba, H. Manome, S. Nakagawa, Z.U. Mollah, M. Mizuashi, T. Ohtani, Y. Yoshino, H. Tagami, p38 Mitogen-activated protein kinase and extracellular signal-regulated kinases play distinct roles in the activation of dendritic cells by two representative haptens, NiCl2 and 2, 4-dinitrochlorobenzene, J. Invest. Dermatol. 120 (2003) 390–399.
[66] S. Nakagawa, T. Ohtani, M. Mizuashi, Z.U. Mollah, Y. Ito, H. Tagami, S. Aiba, p38 Mitogen-Activated protein kinase mediates dual role of ultraviolet B radiation in induction of maturation and apoptosis of monocyte-derived dendritic cells, J. Invest. Dermatol. 123 (2004) 361–370.
[67] S. Agrawal, A. Agrawal, B. Doughty, A. Gerwitz, J. Blenis, T. Van Dyke, B. Pulendran, Cutting edge: different Toll-like receptor agonists instruct dendritic cells to induce distinct Th responses via differential modulation of extracellular signal-regulated kinase-mitogen-activated protein kinase and c-Fos, J. Immunol. 171 (2003) 4984–4989.
[68] A. Puig-Kroger, M. Relloso, O. Fernández-Capetillo, A. Zubiaga, A. Silva, C. Bernabéu, A.L. Corbı, Extracellular signal–regulated protein kinase signaling pathway negatively regulates the phenotypic and functional maturation of monocyte-derived human dendritic cells, Blood, The Journal of the American Society of Hematology 98 (2001) 2175–2182.
[69] E.S. Malsin, S. Kim, A.P. Lam, C.J. Gottardi, Macrophages as a source and recipient of Wnt signals, Front. Immunol. 10 (2019) 1813.
[70] A. Suryawanshi, M.S. Hussein, P.D. Prasad, S. Manicassamy, Wnt signaling cascade in dendritic cells and regulation of anti-tumor immunity, Front. Immunol. 11 (2020) 122.
[71] H. Clevers, Wnt/β-Catenin signaling in development and disease, Cell 127 (2006) 469–480.
[72] L. Wang, J. Li, L.j. Di, Glycogen synthesis and beyond, a comprehensive review of GSK3 as a key regulator of metabolic pathways and a therapeutic target for treating metabolic diseases, Med. Res. Rev. 42 (2022) 946–982.
[73] M. Martin, K. Rehani, R.S. Jope, S.M. Michalek, Toll-like receptor–mediated cytokine production is differentially regulated by glycogen synthase kinase 3, Nat. Immunol. 6 (2005) 777–784.
[74] R.S. Jope, Y. Cheng, J.A. Lowell, R.J. Worthen, Y.H. Sitbon, E. Beurel, Stressed and inflamed, can GSK3 be blamed? Trends Biochem. Sci. 42 (2017) 180–192.